Predicting Malignancy Grade with PET in Non-Hodgkin's Lymphoma

Miriam Rodriguez, Suzanne Rehn, Håkan Ahlström, Christer Sundström and Bengt Glimelius

Departments of Diagnostic Radiology, Oncology and Pathology; and the PET Centre, University of Uppsala, Akademiska Sjukhuset, Uppsala, Sweden

Our goal was to determine whether PET with ^{11}C-methionine and/or ^{18}FDG could predict malignancy grade in non-Hodgkin's lymphoma (NHL). **Methods:** Twenty-three patients with high-grade, low-grade or transformed low-grade NHL were investigated. Standardized uptake values (SUV), transport rate and mass influx values were calculated both for the whole tumor [mean regions of interest, (ROI)] and for the tumor area with the highest levels of activity, comprising four contiguous pixels within each tumor and designated as a hot spot. **Results:** Both ^{11}C-methionine and ^{18}FDG detected all tumors. In addition, ^{18}FDG discriminated between high- and low-grade NHL, whereas ^{11}C-methionine did not. With ^{18}FDG, three transformed low-grade NHLs behaved in an intermediate manner. All quantitative uptake values correlated well with each other for both tracers, except for the mean ROI SUV and transport rate of ^{11}C-methionine. Quantifications of mean ROI uptake and hot spots were strongly correlated. **Conclusion:** The results of this study together with previous findings from other studies indicate that ^{18}FDG but not ^{11}C-methionine can predict malignancy grade in NHL. Further studies with a larger series of patients are needed.

Key Words: positron emission tomography; non-Hodgkin's lymphoma; tumor staging

J Nucl Med 1995; 36:1790–1796

Non-Hodgkin's lymphoma (NHL) consists of heterogeneous groups of neoplasms (*1*). Clinically, there are two major NHL groups: high-grade and low-grade. Within these groupings several subtypes exist; therefore differentiating between low-grade and high-grade NHL is clinically important. Although low-grade NHL is usually considered to be incurable, it often progresses slowly and patients have long survival rates. Treatment is therefore often deferred until symptoms occur and then frequently consists of single-drug cytostatic therapy or radiotherapy if the symptoms are only local. For low-grade NHL, some tumors may have a more aggressive course and some tumors may transform into high-grade NHL (transformed or secondary high-grade NHL). These patients have a poor prognosis. More intensive treatment is given if the disease takes a more progressive course or if transformation occurs (*2*).

In contrast, high-grade NHL has aggressive tumors with high proliferation rates. When the proliferation rates of high- and low-grade NHL were compared, high-grade tumors yielded much higher values, although great variability is seen between and within prognostic groups (*3*). Treatment of high-grade NHL has a curative intention. About 40% of patients can achieve long-term remissions using various combinations of cytostatic agents (*2*).

In most cases, NHL grading is easily made when appropriate biopsy specimens have been taken. In certain patients, great difficulties may be encountered in such sampling. This is particularly evident in cases where the disease is limited to intrathoracic and/or intra-abdominal locations only or when adequate tissue sampling may not easily be accomplished without surgery. Additionally, the transformation of low-grade lymphomas to high-grade ones may occur unpredictably, sometimes requiring multiple sampling for disclosure (*4*). Therefore, in vivo prediction of malignancy grade by an easy and reproducible method would be of great clinical value.

In parallel with increased proliferation, glucose and methionine metabolism and cell membrane transport are usually increased in neoplastic tissue (*5–7*). In head and neck cancer and malignant lymphomas, ^{18}FDG uptake, as analyzed by PET, correlates to proliferation rates (*8,9*).

The potential role of PET for detecting and grading malignant lymphomas and predicting prognoses is limited. Okada et al. (*10*) reported that ^{18}FDG uptake could be useful for prognostic prediction in patients with malignant lymphoma in the head and neck region. In another study, in which ^{11}C-methionine and ^{18}FDG uptake was compared in NHL, Leskinen-Kallio et al. (*11*) found that ^{11}C-methionine was a better tracer for identifying tumors than ^{18}FDG, but ^{18}FDG was superior in predicting malignancy grade (*11*).

The aim of this study was to further evaluate the diagnostic accuracy of PET using ^{11}C-methionine and ^{18}FDG, determining whether either of the tracers could reliably predict the grade of malignancy in NHL.

Received Oct. 21, 1994; revision accepted Apr. 12, 1995.
For correspondence or reprints contact: Miriam Rodriguez, MD, Department of Diagnostic Radiology, Akademiska Sjukhuset, S-751 85 Uppsala, Sweden.

TABLE 1
Patient Characteristics and Clinical Data

Patient no.	Age (yr)	Sex	Malignancy grade	Histology		Stage	CT	MRI	Methionine PET	FDG PET
				Kiel	WF					
1	56	M	High	NUD	NUD	IA	Abdomen	—	—	x
2	55	F	High	NUD	NUD	IIB	Abdomen	Abdomen	x	x
3	70	M	High	d.CB	(G)	IIIA	—	Neck	—	x
4	74	M	High	d.CB	(G)	IVA	Abdomen	—	x	—
5	47	F	High	NUD	NUD	IIB	Abdomen	Abdomen	x	x
6	59	F	High	d.CB	(G)	IIA	Abdomen	Abdomen	x	x
7	63	F	High	d.CB	(G)	IA	Abdomen	—	—	x
8	70	F	High	NUD	NUD	IIB	Abdomen	Abdomen	x	x
9	42	M	High	d.CB	(G)	IIA	Thorax	—	—	x
10	66	M	High	d.CB	(G)	IVB	Neck	Neck	—	x
11	66	M	High	d.CB	(G)	IB	Abdomen	—	—	x
12	73	M	Low	CC	(E)	IVA	Abdomen	—	x	x
13	56	F	Low	CC	(E)	IVB	Abdomen	Abdomen	x	x
14	81	F	Low	NUD	NUD	IIA	Abdomen	—	x	x
15	50	M	Low	f.CB-CC	(B)	IVB	—	Neck	x	x
16	59	M	Low	CLL	(A)	IVA	—	Neck	x	x
17	69	M	Low	CLL	(A)	IVA	—	Axilla	—	x
18	86	M	Low	CLL	(A)	IVA	—	Groin	—	x
19	55	F	Low	f.CB-CC	(B)	IVA	Neck	—	—	x
20	68	M	Low	CLL	(A)	IVA	Groin	—	—	x
21	44	F	Transformed	f+d.CB	(G)	IVB	—	Neck	x	x
22	75	M	Transformed	d.CB	(G)	IVB	Thorax	Thorax	—	x
23	54	M	Transformed	f+d.CB	(G)	IIB	—	Thorax	—	x

NUD = unclassifiable; d.CB = diffuse centroblastic lymphoma; CC = centrocytic lymphoma; CB-CC = centrocytic centroblastic lymphoma; f CB-CC = follicular centrocytic centroblastic lymphoma; CLL = lymphocytic lymphoma; (A) = small lymphocytic; (B) = follicular predominantly small-cleaved cell; (E) = small-cleaved cell; (G) = large cell noncleaved; WF = Working Formulation.

MATERIALS AND METHODS

Patients

We studied 23 patients (14 men, 9 women) who were diagnosed with NHL. Eleven patients had high-grade NHL, 9 low-grade and 3 transformed low-grade (Table 1). All patients had at least one tumor larger than 3 cm in diameter. The high-grade and transformed NHL patients were consecutively enrolled from patients seen between June 1992 and October 1993, whereas the low-grade NHL patients were selected from the patients in the oncology department. The low-grade NHL group consisted of patients with both an indolent and a more rapidly progressive course. Tumors were graded according to the Kiel classification (*1*); a classification was also made according to the Working Formulation (*12*). CT and MRI were performed in all patients for tumor staging in accordance with the Ann Arbor system (*13*) to evaluate a tumor size and determine tumor regions for the PET study (Fig. 1, Table 1). In 10 of the 11 patients with high-grade NHL, PET examinations were performed at the time of diagnosis, prior to any therapy. One patient had a PET study during relapse, which occurred 6 mo after the last chemotherapy course.

Among patients with low-grade NHL, three had PET studies at the time of diagnosis and before treatment was started, and one patient was examined 8 yr after diagnosis but never received any therapy. Five patients had received chemotherapy before the PET examination (four patients were treated with intermittent single-agent therapy and one with combination chemotherapy and/or radiotherapy). One patient had a PET examination 1 mo after the chemotherapy course. None of the other four patients had received any treatment within 5 mo prior to the PET examination.

PET

Patients were examined with a whole-body PET camera that produces 15 simultaneous contiguous axial slices with a slice thickness of 6.5 mm and a resolution of 5–6 mm (*14*). Twenty-two ^{18}FDG PET examinations and 11 ^{11}C-methionine PET examinations were performed. Ten patients were examined with both tracers (Table 1).

All patients fasted for at least 4 hr before the study and the methionine or glucose plasma concentrations were measured before scanning. After a 10-min transmission scan was obtained, the tumor region was imaged after rapid injection of approximately 800 MBq ^{11}C-methionine (*15*) or 400 MBq ^{18}FDG (*16,17*) into a peripheral vein. Immediately after injection, a dynamic scanning sequence was started, consisting of 14 (^{18}FDG) or 16 (^{11}C-methionine) frames with successively increasing acquisition times from 1 to 10 min. During the examination, 13 (^{18}FDG) or 12 (^{11}C-methionine) plasma samples were taken from a peripheral vein, which was arterialized by warming (*18*), and analyzed for ^{11}C or ^{18}F concentration.

Image Reconstruction and Analysis

Image reconstruction produced a set of dynamic images, each representing a quantitative estimate of the radioactivity concentration. A 128 × 128 matrix and a 6-mm Hanning filter were used. Data were corrected for attenuation and scatter (*19*). Carbon-11-methionine data were obtained from 14 to 45 min and ^{18}FDG data were obtained from 30 to 50 min postinjection and summed to produce an average image.

The radioactivity concentration in the average image was re-

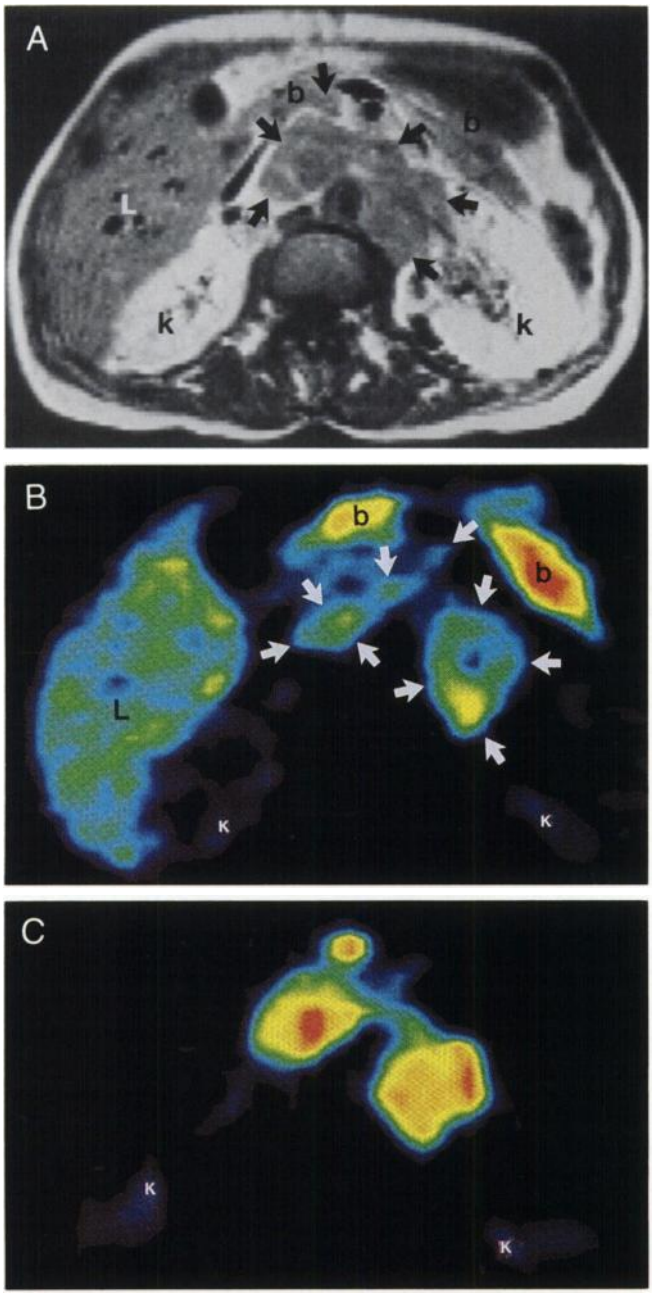

FIGURE 1. Axial MRI and PET images of the abdomen at corresponding levels in a patient with high-grade NHL. (A) MRI T1-weighted image obtained after intravenous injection of gadolinium contrast depicts a large central tumor (arrows). L = liver, k = kidney, b = bowel. (B) PET ^{11}C methionine SUV image visualizes tracer uptake in the tumor (arrows), liver (L), kidneys (k) and bowel (b). Red and yellow colors correspond to high tracer uptake. (C) PET ^{18}FDG SUV image visualizes tracer uptake in the tumor and kidneys (k). Red and yellow colors correspond to high tracer uptake.

calculated to provide images of standardized uptake values (SUV): The concentration of radioactivity in the lesion was divided by the ratio of totally administered radioactivity to body weight.

Quantitative analyses were also performed on a pixel-by-pixel basis according to the technique described by Patlak et al. (*20*), generating images of tracer transport rate in tissues using plasma radioactivity as a reference. Because we were unable to perform individual analyses of methionine metabolites, a standard correction for metabolites calculated from data presented by Hatazawa et al. (*21*) was applied to the plasma data. Hatazawa et al., however, recommend individual metabolite analyses.

For the SUV images, regions of interest (ROIs) representing viable tumor areas with the highest radioactivity were drawn according to a standardized procedure. This meant that in drawing a ROI, a contour positioned halfway between the highest tumor radioactivity and the surrounding tissues was followed. From each ROI obtained in this manner (designated as mean ROI), the mean tumor radioactivity value could be obtained. In addition to this mean ROI, a region within each tumor comprising the four contiguous pixels with the highest levels of activity and designated hot spot was identified. Thus, corresponding SUVs and transport rate values were estimated.

The transport rate values obtained for the mean ROI and the hot spot were multiplied by plasma level values of methionine and glucose, with a lumped constant of 0.4 (measured for the normal brain and used in this study because the lumped constant for lymphoma is unknown) (*22*) for each patient to estimate the mass influx of methionine [nmole/(mlmin)] and glucose [μmole/(100 mlmin)], respectively in the tumor area.

Statistical Methods

Differences in the distribution of values between the two groups were assessed with the Mann-Whitney U-test. Correlation between different parameters was measured with the Spearman Rank correlation test. These analyses were performed with Stat View II (Stat View™ 1986) on a Macintosh computer.

RESULTS

All tumors detected by CT or MRI were clearly visualized by ^{11}C-methionine and/or ^{18}FDG (Figs. 2, 3). The uptake values of ^{11}C-methionine and ^{18}FDG for patients in each group, quantified as SUV, transport rate and mass influx, are shown in Figures 2 and 3, respectively. Mean values for the mean ROIs and hot spot, respectively, are presented in Table 2.

The different quantitative tracer values correlated well with the hot spot (data not shown). Good correlation was also found for the mean ROI, with the exception of the methionine transport rate SUV (Figs. 4, 5).

The uptake values for ^{18}FDG were significantly higher for high-grade than low-grade NHL, whether recorded as SUV ($p < 0.01$), transport rate ($p < 0.003$) or mass influx ($p < 0.01$). No such significant difference was seen for ^{11}C-methionine uptake values (SUV $p = 0.9$, transport rate $p = 0.1$, mass influx $p = 0.2$). Uptake values varied considerably within the two prognostic groups, irrespective of the estimation method. For ^{18}FDG, there were no overlapping values between high-grade and low-grade NHL for transport rate, whereas this was the case for both SUV and mass influx estimations (Fig. 3). The few patients with transformed NHL had uptake values that behaved in an intermediate manner. In the transport rate calculations for ^{18}FDG, two patients with transformed lymphomas had values higher than those of all low-grade tumors that fell within the range of the high-grade values. No such clear

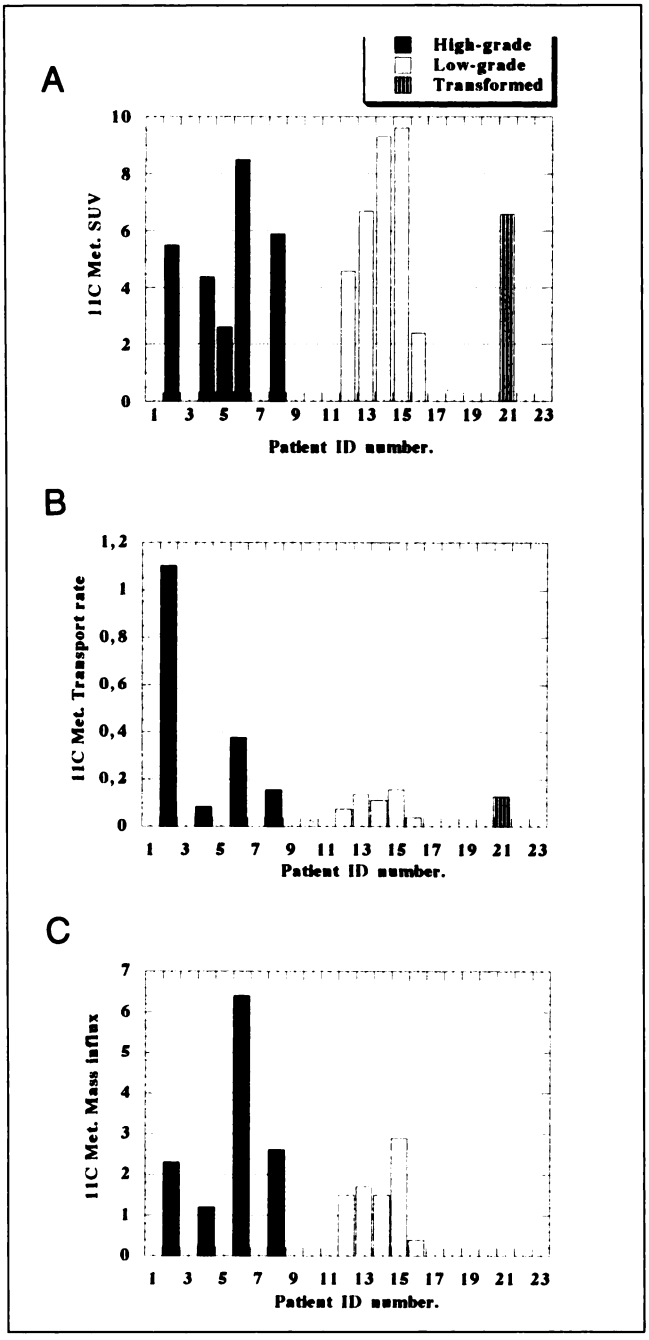

FIGURE 2. Uptake of ^{11}C-methionine in patients with high-grade, low-grade and transformed low-grade NHL quantified with (A) SUV, (B) transport rate (min^{-1}) and (C) mass influx [nmole/(ml · min)].

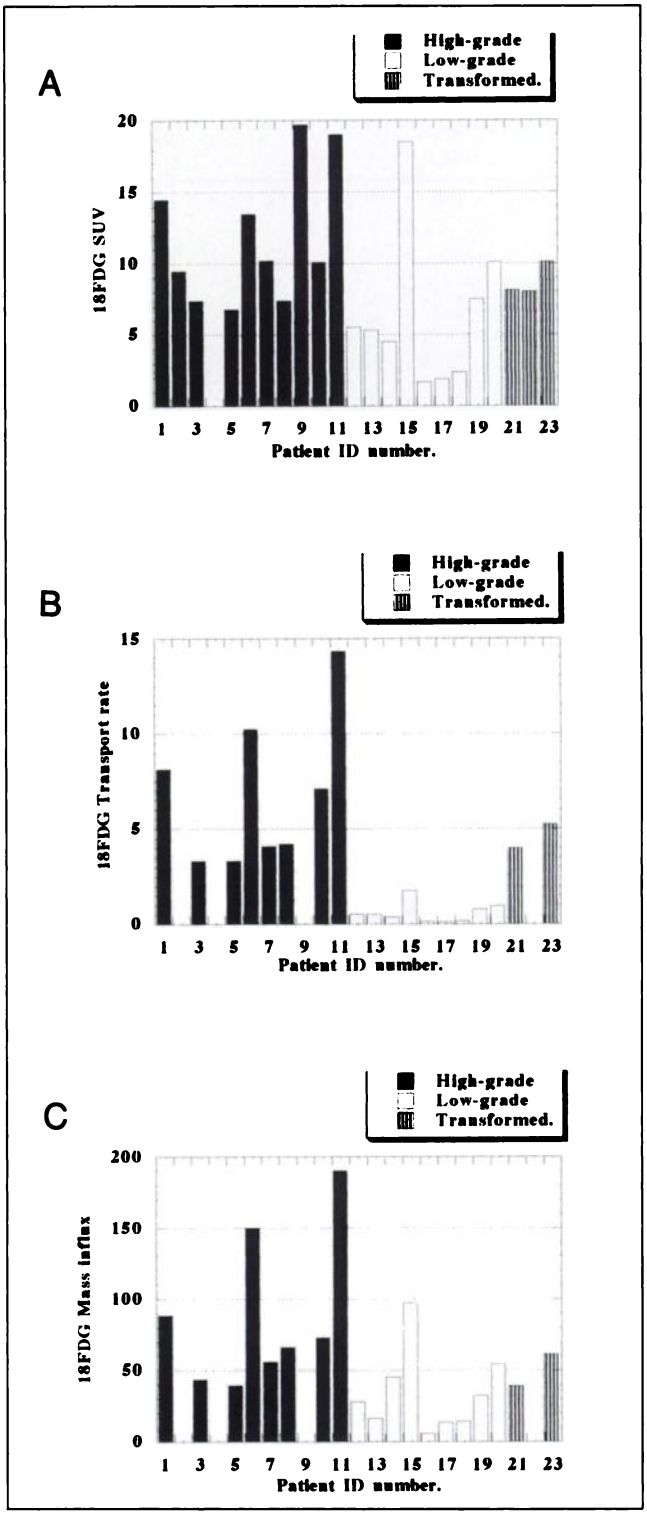

FIGURE 3. Uptake of ^{18}FDG in each patient with high-grade, low-grade and transformed low-grade NHL quantified with (A) SUV, (B) transport rate (min^{-1}) and (C) mass influx [μmole/(100 ml · min)].

difference was detected for ^{11}C-methionine (Fig. 2B), but only one patient with transformed NHL was studied.

DISCUSSION

This study showed that both ^{11}C-methionine and ^{18}FDG, as nonspecific tracers for metabolic activity, have high sensitivity for detecting malignant lymphomas. Our results differ from those reported by Leskinen-Kallio et al. (*11*), who found that low-grade NHL may not always be visualized on ^{18}FDG PET images, whereas they are visualized on ^{11}C-methionine images. Leskinen-Kallio et al. (*11*) detected tumor location for the PET studies by palpation (except for one case of abdominal lymphoma where CT was performed). We, however, consistently performed CT and/or MRI to determine tumor regions. Although Leski-

TABLE 2
Quantitative Uptake Values Related to Malignancy Grade

Malignancy grade	^{11}C Met/M. ROI SUV	^{11}C Met/M. ROI T. rate (min^{-1})	^{11}C Met/M. ROI Mass. i [nmole/(ml · min)]	^{11}C-Methionine hot spot SUV	^{11}C-Methionine hot spot T. rate (min^{-1})	^{11}C-Methionine hot spot Mass. i [nmole/(ml · min)]
High grade mean ± s.d.	5.38 ± 2.16	0.428 ± 0.465	3.12 ± 2.26	8.88 ± 2.87	0.257 ± 0.187	4.50 ± 3.15
Low grade mean ± s.d.	6.52 ± 3.07	0.103 ± 0.047	1.60 ± 0.88	8.50 ± 3.54	0.126 ± 0.059	2.00 ± 1.18
Transformed mean ± s.d.						

	^{18}FDG/M. ROI SUV	^{18}FDG/M. ROI T. rate (min^{-1})	^{18}FDG/M. ROI Mass. i [μmole/(ml · min)]	^{18}FDG hot spot SUV	^{18}FDG hot spot T. rate (min^{-1})	^{18}FDG hot spot Mass. i [mole/(μml · min)]
High grade mean ± s.d.	11.8 ± 4.70	6.83 ± 3.94	88.2 ± 53.9	15.90 ± 5.71	9.37 ± 5.09	122.0 ± 70.3
Low grade mean ± s.d.	6.37 ± 5.30	0.60 ± 0.52	34.2 ± 28.4	8.70 ± 6.60	2.64 ± 2.77	47.8 ± 36.8
Transformed mean ± s.d.	8.73 ± 1.18	4.59 ± 0.87		11.60 ± 1.74	6.19 ± 1.18	

SUV = standardized uptake value; T. rate = transport rate; Mass. i = mass influx; M. ROI = mean region of interest.

nen-Kallio et al. (*11*) used ROIs with at least 43 pixels, our study used a standardized procedure to draw a mean ROI to represent only the viable tumor area that could be taken from the CT and/or MRI image. The use of a strictly defined ROI may be a way to avoid nondetection caused by, for example, necrosis in the tumor. We cannot further explain the apparent discrepancies between the two studies partly because the level of description in the Leskinen-Kallio study is not always sufficient for further comparison.

In our study, ^{18}FDG could discriminate between low-grade and high-grade NHL. This discrimination was apparently better when transport rate calculation was used instead of SUV or mass influx estimations. In actuality, the transport rate value discriminated entirely between prognostic groups without any overlapping values. Because our patient population is small; this result should be interpreted cautiously.

On the other hand, ^{11}C-methionine had no discriminative ability. Although group differences may exist, we noted overlapping values irrespective of the calculation method. Our findings are also supported by the results of Leskinen-Kallio et al. (*11*), who detected no discriminative ability of ^{11}C-methionine.

DiChiro (*23*) studied patients with malignant glioma and found a similar ability of ^{18}FDG to discriminate between malignancy grades. In studies of other tumor types, however, in which the patient populations are usually small, overlapping values between different malignancy groups have been reported for ^{11}C-methionine and ^{18}FDG uptake (*11,24*).

There have been few comparisons of SUV, transport rate and mass influx estimations in the same study (*9*). No firm conclusions can be drawn as to whether the less resource demanding SUV method is sufficient for quantitating tracer uptake in lymphomas or other tumors. In our study, transport rate estimations appeared to be advantageous. In Patient 15, who had a low transport rate value (Figs. 2B, 3B) but a high SUV (Figs. 2A, 3A) despite a low-grade histology, the PET study was actually repeated after 6 mo with virtually identical results. During that time, no treatment was given and there was no lymph node enlargement and a new biopsy showed the same histological subtype.

From a clinical view, tumor detection and clearly distinguishing in vivo between low-grade and high-grade NHL with one tracer, ^{18}FDG, is promising. There are, however, clinical considerations. For many reasons PET is not widely available. Therefore, for more readily available and accessible methods are needed. Computed tomography and ^{67}Ga scintigraphy have been extensively used for tumor staging, but neither method can distinguish between grades. In this context, heterogeneity investigations using MRI have, shown promising results (*25,26*). Gallium-67 scintigraphy also reportedly has a lower sensitivity for detecting low-grade NHL (*27,28*).

PET imaging with nonspecific tracers may, however, be of importance for other clinical purposes. For example, it may illustrate important differences between low- and high-grade NHL that could direct future diagnostic, and possibly, therapeutic studies. The ability to reflect metabolic/proliferative activity, as also found by Okada et al. (*9*), may provide helpful data in predicting early treatment response of malignant lymphomas. In a comparative study,

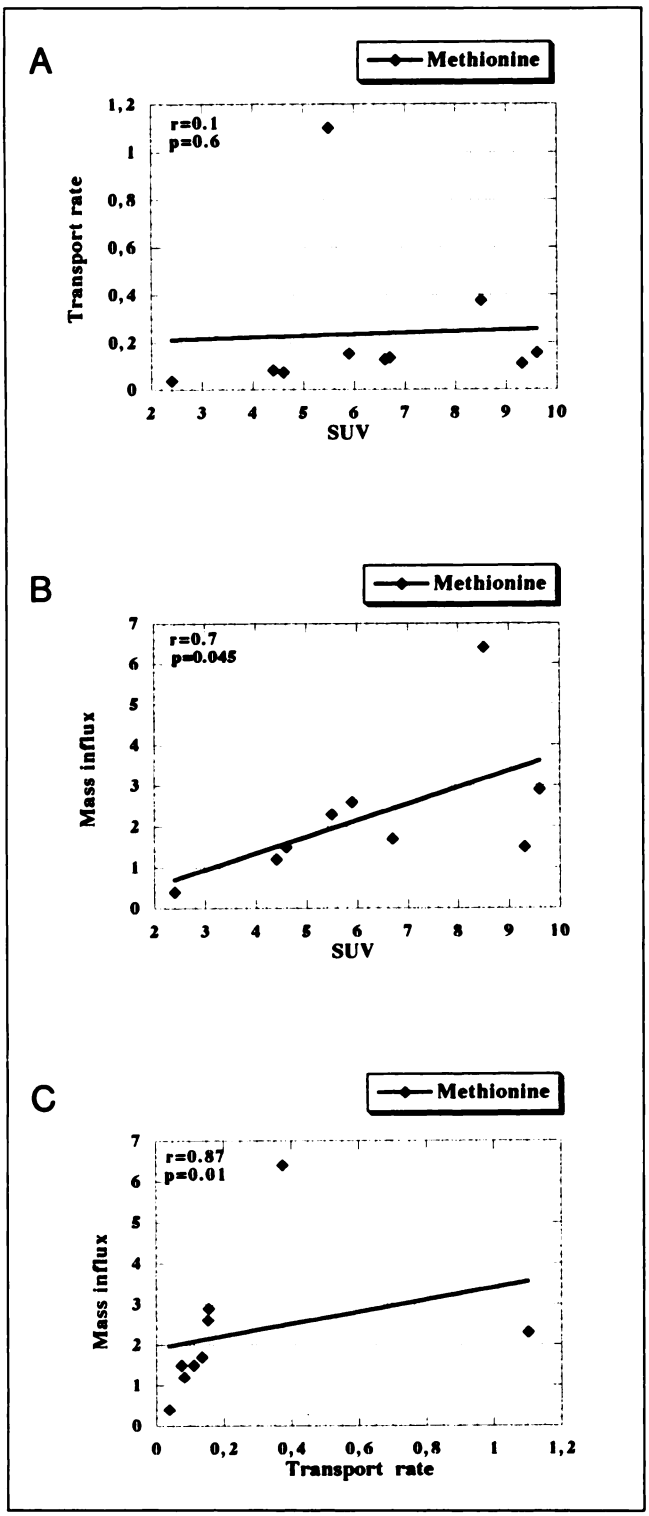

FIGURE 4. Correlations between ^{11}C-methionine (A) transport rate (min^{-1})/SUV, (B) mass influx [nmole/(ml · min)]/SUV and (C) transport rate (min^{-1})/mass influx [nmole/(ml · min)], respectively.

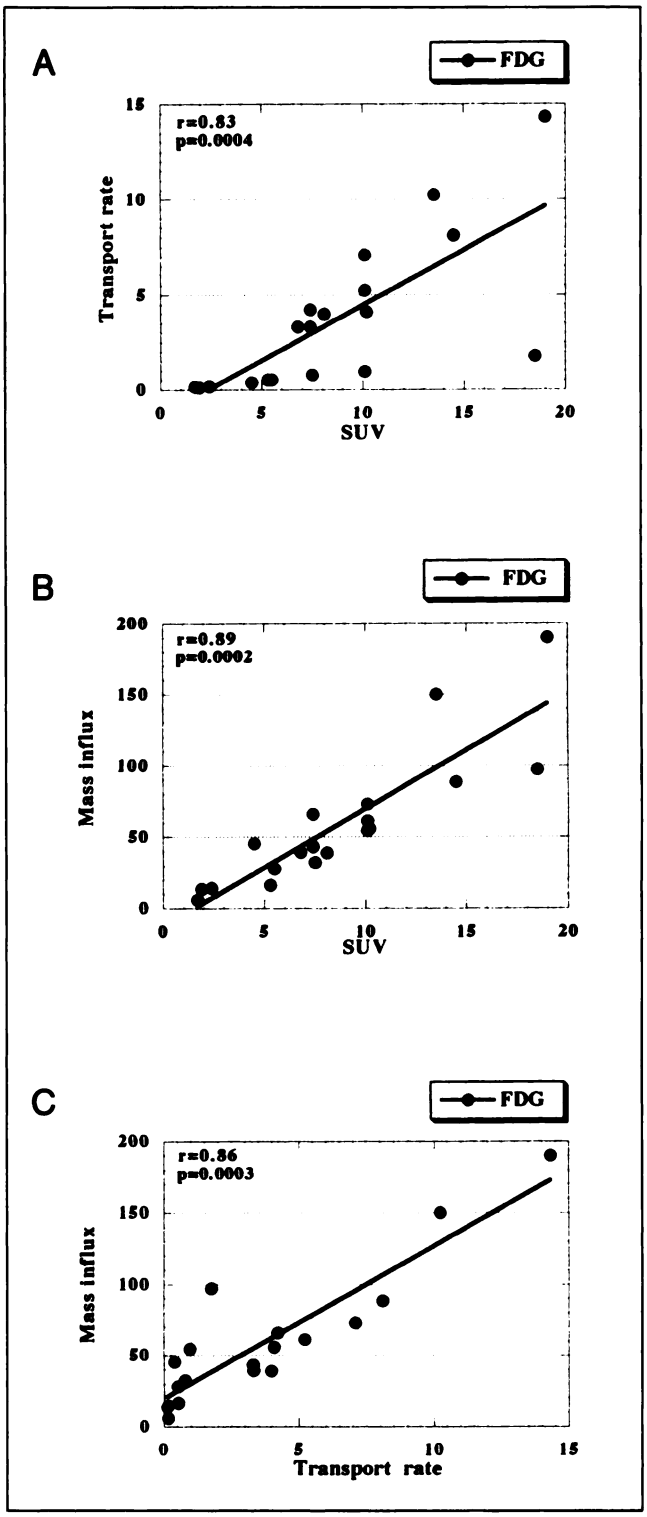

FIGURE 5. Correlation between (A) ^{18}FDG transport rate (min^{-1})/SUV, (B) mass influx [μmole/(100 ml · min)]/SUV and (C) transport rate (min^{-1})/mass influx [μmole/(100 ml · min)], respectively.

the correlation with metabolic state was superior for ^{18}FDG compared to ^{67}Ga scintigraphy (*10*). Hoekstra et al. (*29*) found that these two methods reflected functional activity equally well, but that ^{18}FDG imaging appeared superior to ^{67}Ga in predicting early response. Also, the ability to discriminate between remaining active tumor cells and fibrotic tissue in residual mass after treatment may be possible. Gallium-67 imaging has been reported to be useful in assessing prognosis after therapy (*30*) and evaluating tu-

mor viability in residual masses (*31,32*). In the study by Hoekstra et al. (*29*), neither planar ^{18}FDG nor ^{67}Ga imaging could exclude remaining viable tumor. Hoekstra et al. postulate that PET may provide clinically relevant information due to its superior detection capacity in these patients.

CONCLUSION

Future PET research should focus on developing more specific tracers as well as clinically important issues in assessing patients with malignant lymphoma. For selected indications or sites where other imaging methods are insufficient for diagnostic and staging purposes, PET may have a limited but definitive role.

ACKNOWLEDGMENTS

This work was supported by grants from the Swedish Cancer Society and from the University Hospital, Uppsala, Sweden.

REFERENCES

1. Lennert K. Malignant lymphomas other than Hodgkin's disease. In: *Handbuch der speziellen plathologischen Anatomie und Histologie*. Berlin: Springer-Verlag: 1978:84.
2. Armitage JO. Drug therapy: treatment of non-Hodgkin's lymphoma. *N Engl J Med* 1993;328:1023–1030.
3. Rehn S, Glimelius B, Sundström C. A comparative study of proliferation-associated parameters in B-cell non-Hodgkin lymphomas. *Hematol Oncol* 1991;9:287–298.
4. Hoppe RT. Histologic variation in non-Hodgkin's lymphomas: commentary. *Cancer Treat Rep* 1981;11–12:935–939.
5. Gallagher BM, Fowler JS, Gutterson NI, et al. Metabolic trapping as a principle of radiopharmaceutical design: some factors responsible for the biodistribution of (^{18}F)2-deoxy-2-fluoro-D-glucose. *J Nucl Med* 1978;19: 1154–1161.
6. Hoffman RM. Altered methionine metabolism DNA methylation and oncogenic expression in carcinogenesis. *Biochem Biophys Acta* 1984;738:49–87.
7. Stern PH, Wallace CD, Hoffman RM. Altered methionine metabolism, occurs in all members of a set of diverse human tumor cells lines. *J Cell Physiol* 1984;119:29–34.
8. Minn H, Joensuu H, Ahonen A, Klemi P. Fluorodeoxyglucos imaging: a method to assess the proliferative activity of human cancer in vivo. Comparison with DNA flow cytometry in head and neck tumors. *Cancer* 1988; 61:1776–1781.
9. Okada J, Yoshikawa K, Itami M, et al. Positron emission tomography using fluorine-18-fluorodeoxyglucose in malignant lymphoma: a comparison with proliferative activity. *J Nucl Med* 1992;33:325–329.
10. Okada J, Yoshikawa K, Imaseki K, et al. The use of FDG-PET in the detection and management of malignant lymphoma: correlation of uptake with prognosis. *J Nucl Med* 1991;32:686–691.
11. Leskinen-Kallio S, Ruotsalainen U, Någren K, Teräs M, Joensuu H. Uptake of carbon-11-methionine and fluorodeoxyglucose in non-Hodgkin's lymphoma: a PET study. *J Nucl Med* 1991;32:1211–1218.
12. Rosenberg SA, Berard CW, Brown BW, et al. National Cancer Institute sponsored study of classification of non-Hodgkin's lymphomas: summary and description of a working formulation for clinical usage. *Cancer* 1982; 49:2112–2135.
13. Carbone PP, Kaplan HS, Musshoff K, Smithers DW, Tubiana M. Report of the committee in Hodgkin's disease staging classification. *Cancer Res* 1971; 31:1860–1861.
14. Kops ER, Herzog H, Schmid A, Holte S, Feinendegen LE. Performance characteristics of an eight-ring whole-body PET scanner. *J Comput Assist Tomogr* 1990;14:437–445.
15. Långström B, Halldin C, Antoni G, et al. Synthesis of L- and D- [methyl-^{11}C]-methionine. *J Nucl Med* 1987;28:1037–1040.
16. Hamacher K, Coenen HH, Stöcklin G. Efficient stereospecific synthesis of no-carrier-added 22-(^{18}F)-fluoro-2-deoxy-D-glucose using aminopolyether supported nucleophilic substitution. *J Nucl Med* 1986;27:235–238.
17. Toorogian SA, Mulholland GK, Jewett DM, et al. Routine production of 2-deoxy-2-(^{18}F) fluoro-D-glucose by direct nucleophilic exchange on a quaternary 4-aminopyridiunium resin. *Int J Rad Appl Instrum* 1990;17:273–279.
18. Abumrad NN, Rabin D, Diamond MP, Lacy WW. Use of a heated superficial hand vein as an alternative site for the the measurement of amino acid concentration and for the study of glucose and alanine kinetics in man. *Metabolism* 1981;30:936–940.
19. Bergström M, Eriksson L, Bohm C, Blomqvist G, Litton J. Correction for scattered radiation in a ring detector positron camera by integral transformations of the projections. *J Comput Assist Tomogr* 1983;7:42–50.
20. Patlak CS, Blasberg RG, Fenstermacher JD. Graphic evaluation of blood-to-brain transfer constants from multiple-time uptake data. *J Cereb Blood Flow Metab* 1983;3:1–7.
21. Hatazawa J, Ishiwata K, Itoh M, et al. Quantitative evaluation of L-(methyl-C-11)-methionine uptake in tumor using positron emission tomography. *J Nucl Med* 1989;30:1809–1813.
22. Kuwabara H, Evans AC, Gjedde A. Michaelis-menten constraints improved cerebral glucose metabolism and regional lumped constant measurements with (^{18}F) fluorodeoxyglucose. *J Cereb Blood Flow Metab* 1990;10: 180–189.
23. DiChiro G. Positron emission tomography using (^{18}F) fluorodeoxyglucos in brain tumors: a powerful diagnostic and prognostic tool. *Invest Radiol* 1986;22:360–371.
24. Strauss LG, Conti PS. The applications of PET in clinical oncology. *J Nucl Med* 1991;32:623–648.
25. Rehn S, Nyman R, Glimelius B, Hagberg H, Sundström C. Magnetic resonance imaging for predicting prognostic grade in non-Hodgkin lymphomas. *Radiology* 1990;176:249–253.
26. Rehn S, Sperber G, Nyman R, Glimelius B, Hagberg H, Hemmingsson A. Quantification of inhomogenieties in malignancy grading of non-Hodgkin lymphomas with MR imaging. *Acta Radiol Diagn* 1993;34:3–9.
27. Longo DL, Schilsky RL, Blei L, Cano R, Johnston GS, Young RC. Gallium-67 scanning: limited usefulness in staging patients with non-Hodgkin's lymphoma. *Am J Med* 1980;68:695–700.
28. Larcos G, Farlow DC, Antico VF, Gruenewald SM, Boyages J. The role of high dose ^{67}Ga scintigraphy in staging untreated patients with lymphoma. *Aust NZ J Med* 1994;24:5–8.
29. Hoekstra OS, Ossenkoppele GJ, Golding R, van Lingen A, Visser GWM, Teule GJJ, Huijgens PC. Early treatment in malignant lymphoma as determined by planar fluorine-18-fluorodeoxyglucose scintigraphy. *J Nucl Med* 1993;34:1706–1710.
30. Israel O, Front D, Lam M. Gallium-67 imaging in monitoring lymphoma respons to treatment. *Cancer* 1988;61:2439–2443.
31. Israel O, Front D, Epelbaum R. Residual mass andnegativ gallium scintigraphy in treated lymphoma. *J Nucl Med* 1990;31:365–368.
32. Joshua DE, McLaughlin AF, Kronenberg H, et al. Residual mass and gallium scanning [Letter]. *J Clin Oncol* 1989;7:144–145.